Soil Dynamics & Earthquake Engineering Conference / Southampton / 1982.07.13-15

Centrifugal Testing of Microconcrete Retaining Walls Subjected to Base Shaking

M.D.BOLTON & R.S.STEEDMAN
Cambridge University, UK

1. INTRODUCTION

1.1 Background

It is widely recognised that the proper design of earth retaining structures is essential in regions at risk from earthquakes. The lifelines which will bring relief in the immediate aftermath of an earthquake depend on the integrity of port facilities such as quay walls and highway structures such as bridge abutments and walls which have been used to retain slopes or create separations of grade. The classical wedge analysis of gravity walls by Okabe (1926) and Mononobe and Matsuo (1929) has been available for 50 years. Recent refinements of this technique by Elms and Richards (1979), following the method of Newmark (1965), have sought to predict the displacements of gravity retaining walls which are free to slide on a rigid horizontal surface, and subjected to base shaking. These calculations have performed well in relation to the behaviour of small models reported by Lai Cho Sim and Berrill (1979).

There is little published information on the overall sliding, settling and rotation of gravity retaining walls subject to general seismic displacements. Many retaining walls have functional requirements that would preclude large deformation. Rail tracks frequently run beside quay walls, and bridge abutments must be designed in such a way that the deck is offered continuing support should the abutments separate whilst being protected from buckling in the event of the supports approaching. Many designers may therefore elect to employ cantilever walls with fixed foundations. Their outstanding problem is then to ascertain the relevance of the classical wedge calculation to deformation and damage of fixed-base structures.

Wood (1972) and (1975) has considered the theoretical behaviour of rigidly founded retaining walls, adapting the

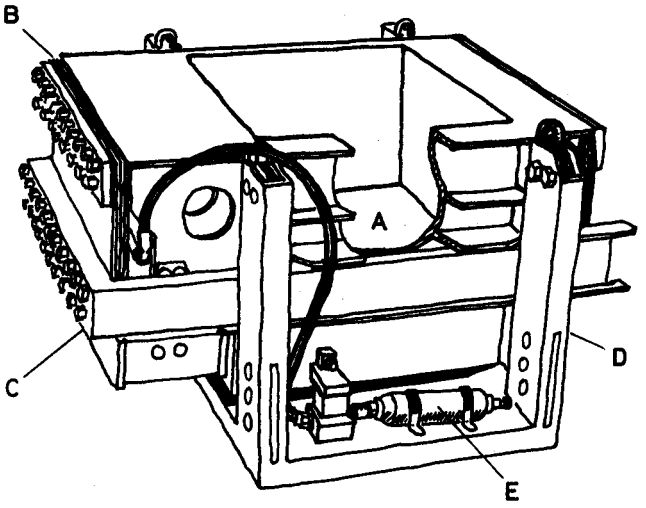

(a) THE MORRIS BOX

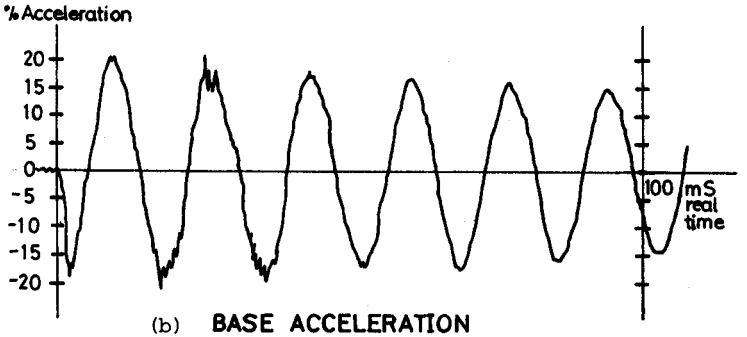

(b) BASE ACCELERATION

SPECIMEN CONTAINER ——— A
STEEL PLATE SPRINGS ——— B
RING BEAM (REACTION MASS) ——— C
SUSPENSION FRAME ——— D
HYDRAULICS TO RELEASE CATCH ——— E

Fig. 1 The Morris Box

finite element technique for the purpose. His work has pointed to the need for reliable data of elastic shaking interactions being modified as higher lateral accelerations cause irreversible strains leading ultimately to collapse. Ortiz Scott and Lee (1981) have recently reported tests in which a very flexible aluminium model wall, retaining dry sand in a centrifugal container, has been subjected to base shaking. The subject of this paper is a similar style of test on micro-concrete cantilever walls tested on the Cambridge Geotechnical Centrifuge.

1.2 Modelling criteria

The essence of centrifugal model testing lies in the use of materials similar to those employed in the field, formed in similar geometries with every dimension in the model reduced by the scaling factor n, and the model subjected to centripetal accelerations n times earth's gravity. Boundary conditions should be replicated as closely as possible in terms of stress or scaled displacement. Schofield (1980) shows that lateral shaking in the field can be modelled in the centrifuge by inducing displacements scaled down by the factor n at shaking frequencies scaled up by n, so that lateral accelerations are correctly scaled up by n in the model.

The specific objective of the tests reported here was to observe and classify the behaviour of reinforced concrete cantilever walls with granular backfill, subjected to simplified earthquakes of various intensities. It was considered desirable to fulfill the ideal requirements of structural modelling as closely as possible in these pilot tests. Dynamic behaviour is a function of density, stiffness, strength and ductility, and it was therefore decided to attempt the construction of reinforced micro-concrete models with properties as representative as possible of those of full scale structures. Although it was recognised that the liquefaction of loose sands beneath the water table was a significant problem in waterfront structures, it was decided to focus the initial tests on the simpler problem of dry granular backfill.

The experiment was conducted using the shaking table developed by Morris (1979) and depicted schematically in Figure 1(a). The shaking is provided by the mass of the soil model and its container vibrating against a reaction mass connected to it by stiff leaf springs. This assembly is hung by a flexible suspension from an outer frame, so that the counteracting inertial forces are well isolated from the rotor. The whole package is bolted to the standard swinging platform, described by Schofield (1980). To prime the box the two masses are jacked apart with a hand pump while the rotor is stationary and a metal catch is inserted. Hydraulic jacks are used to activate the catch when the desired centrifuge speed has been attained. The amplitude of the vibration is controlled by the thickness of the insert, and various lateral accelerations between 5 and

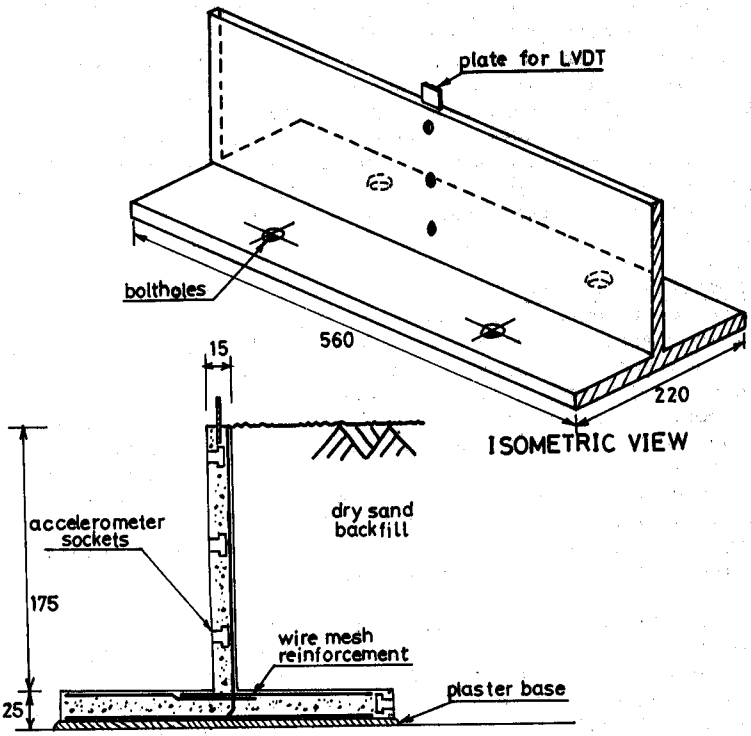

Fig. 2(a) Microconcrete T-section retaining walls

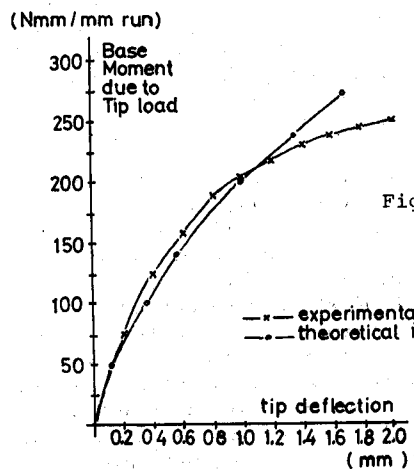

Fig. 2(b) Experimental results for tip load compared with equation 3.

18 g were achieved in the pilot tests, which were all run at a centrifugal acceleration of 80g, implying lateral acceleration coefficients of 6 to 22%.

The frequency of vibration was about 60 Hz which was therefore equivalent to 60/80 = 0.75 Hz at full scale. However, Figure 1(b) demonstrates that the earthquake signature, comprising a sine wave with very little damping, is quite unlike the complex excitation of a typical earthquake. The chief advantage of the simpler excitation is that it is repeatable, and more easily subjected to real-time analysis than would otherwise be the case. A disadvantage, obviously, is that a given model should ideally be subjected to a number of different forcing frequencies, if the experimenter is to be confident that all possible resonances have been fully explored. The lack of vertical accelerations, common to most model shaking experiments, might have been an equally important omission if the replication of field effects were to have been the sole objective. It was decided, however, that the relevance of classical earthquake calculations to fixed-base retaining walls could validly be assessed with the simplified excitations since the classical methods make use only of the extreme accelerations. The total energy released in a single shaking is easily computed from the imposed deflection of the leaf springs, and lies in the range 0 - 80 J. This would correspond at full scale to incident energy of up to 0.9 MJ/m along the wall.

1.3 Model Technology

The ambition of a retaining wall designer is to achieve a structure which can survive the full range of construction and operational conditions, including earthquakes, which might reasonably be anticipated for it, without lapsing into any 'limit state'. The objective of this research study was on the other hand, to subject model walls to simplified earthquakes which would result in limit states being achieved, whether of excessive deflection, cracking, or collapse. If limit state events can be observed, categorised and made predictable, designers should then be able to steer a more precise course between conservatism and economy. It would therefore have been counterproductive only to create model walls which possessed large 'factors of safety'.

The microconcrete models were of an inverted-T form shown in Figure 2(a). The lower flange was bolted rigidly to the shaking table through a plaster envelope, which was used to create a good seat. The stem of the wall was 175 mm high representing, at the selected acceleration of 80g, a field-scale structure 14 m high. Walls were produced with stem thickness of 35 mm, 24 mm and 15 mm (corresponding at full scale to 2.8 m, 1.9 m and 1.2 m). The concrete was made with rapid hardening Portland cement, and fine-medium sand at an aggregrate/cement ratio 2.5 and with a water cement ratio of 0.54. The reinforcement was standard mild steel wire mesh which was heat treated to

improve its ductility. The 15 mm wall, some results from which will be introduced below, was reinforced with a sheet of 22 gauge ¼ inch (6.3 mm) mesh in the stem and 16 gauge ½ inch (12.7 mm) mesh in the base. Plaster spacers were used to hold the mesh off the shutters and threaded brass sockets were cast in, as shown in Figure 2(a), to receive accelerometers. The shutters were removed 7 hours after casting to prevent shrinkage cracks.

As each model wall was cast, a 100 mm long test-piece of identical section was also produced. This was subjected to a static cantilever bending test to destruction in the laboratory, shortly after the model wall had been tested in the centrifuge. Figure 2(b) contains data of base moment versus tip deflections for the 15 mm wall. This procedure, together with the routine tensile testing of reinforcement and the crushing of cylinder samples of various ages, was essential to the control and calibration of the models, since concrete at small scales is potentially even more variable in its stress-strain properties than it is at larger scales. There is a well-known problem with reinforcement bond in microconcrete but it was considered that the use of mesh would obviate slippage. This was borne out after tests to failure, when the desired 'under-reinforced' behaviour - tensile cracking of the concrete, yield of the reinforcement, large rotations with eventual necking, and rupture of the reinforcement exposed in the tension crack - was observed.

Although it was considered important for similitude to subject the test-piece to cantilever bending action it was recognised that the base moment/tip deflection relation for the centrifuged wall would be a function of the actual stress distribution. Large strain bending behaviour is usually represented hyperbolically:

$$\frac{1}{M_p} + \frac{R}{B_e} = \frac{1}{M} \qquad (1)$$

where M is the bending moment, R the radius of curvature, B_e the initial elastic bending stiffness EI (observed when R is large), and M_p the peak moment of resistance (observed when R is small). A good fit to the tip-loading data of the 15 mm thick wall shown in Figure 2(b) was obtained with values $B_e = 4.8$ kNm^2/m and $M_p = 0.29$ kNm/m.

Equation (1) can be written, for small curvatures $\frac{d^2y}{dx^2} = {}^1/_R$,

$$M = \frac{B_e \frac{d^2y}{dx^2}}{\left(1 + \frac{B_e}{M_p}\frac{d^2y}{dx^2}\right)} \qquad (2)$$

This might be a convenient relationship for the deduction of bending moments from data of bending strains ε measured at some distance b from the neutral axis, so that $\frac{d^2y}{dx^2} = \varepsilon/b$. It is, however, unwieldy for the purposes of double integration with arbitrary distributions of moment which are required if deflections are to be predicted in the general case.

A simplified analagous expression

$$M = \frac{B_1 \frac{d^2y}{dx^2}}{\left(1 + \frac{M}{M_1}\right)} \qquad (3)$$

is much easier to integrate, and can be seen in Figure 2(b) to offer an adequate fit to the cantilever test data of the 15 mm wall up to about 1.5 mm deflection (1.5° average wall rotation) with constants B_1 = 6.0 kNm^2/m and M = 0.08 kNm/m. It must be remembered that the non-linearity evident in Figure 2(b) offers a further latent difficulty of interpretation in that a dynamic cycling load with a mean value at some point along the loading curve would initially excite a loading response along the tangent to the curve and then an unloading and reloading response at a gradient similar to the initial elastic loading gradient B. For wall tip deflections in the range 2 mm to rupture (circa 10 mm) the best idealisation is of a plastic hinge with a loading capacity of 0.29 kNm/m dissipating energy at the rate of about 0.9 J/mm of tip deflection, but subject to elastic recovery on unloading.

The soil which was used as the experimental fill was 14-25 Leighton Buzzard sand, poured nominally dry from a hopper. Density could be varied by altering the rate of flow and height of drop: dense samples reported here had a void ratio of about 0.55, and loose samples about 0.75. Data from plane strain tests on this sand in the simple shear apparatus reported by Stroud (1971) indicate that the peak static angles of shearing resistance should be 53° (dense) and 41° (loose) at low stress levels, reducing to 49° (dense) and 38° (loose) at stresses corresponding to the base of the centrifugal models. The angles of shearing mobilized at 1% shear strain were roughly 40° (dense) and 28° (loose). The critical state angle of shearing resistance after large deformation is of the order 33°. Morris (1979) produced data of dynamic shear modulus of the same sand at a void ratio of 0.65, up to strain amplitudes of 10^{-4}, and at various confining pressures in a resonant column apparatus. These data can be expressed approximately for the purposes of the centrifuge models at 80g as $G = 300\ Z^{\frac{1}{2}}$ MN/m^2 where Z is the depth in metres beneath the sand surface.

2 Theoretical modes of behaviour

2.1 Elastic waves

The speed of propagation of shear waves in an elastic medium is $Vs = \sqrt{G/\rho}$ which leads approximately to $Vs = 420\ Z^{\frac{1}{4}}$ m/s as the vertical speed of propagation of shaking from the base of the sand. The delay through 200 mm depth of sand would then, by integration, be roughly 1 millisecond.

The speed of propagation of plane compression waves is $Vp = \sqrt{Eo/\rho}$ where Eo is the constrained elastic modulus, leading to $Vp \simeq 2Vs$. The distance between the test-wall and the end-wall of the shaking container was 350 mm, so that the delay in the reception by the test-wall of p-waves transmitted from the end-wall would also be approximately 1 millisecond.

An estimate of the phase velocity of transverse waves along an elastic cantilever may be deduced from Graff (1975) to be

$$Vb \simeq \frac{0.746}{L}\sqrt{\frac{EI}{\rho A}}$$

On substituting L = 0.175 m, $EI = B_e = 4.8$ kNm^2/m, $\rho = 2300$ kg/m^3 and $A = 0.015$ m^2/m for the 15 mm microconcrete wall, the velocity Vb is found to be 50 m/s, which would lead to a 3.5 millisecond delay between the base and crest of the cantilever, if it were isolated.

The cyclic period of the model excitation is roughly 16 milliseconds which is substantially longer than the time delay of about 1 millisecond at the crest of the wall arising out of a consideration of the speed of propagation of elastic waves in the materials. If it were thought that the dominant mode of energy transmission were shear waves in the sand, a phase delay corresponding to roughly $\frac{1}{16}$ of a cycle or roughly 25° might be expected over the height of the cantilever wall. Converting the velocities to natural frequencies in first modes, and characterising the shear wave velocity in the sand as constant at its average value of 175 m/s, we obtain natural frequencies of 250 Hz for lateral shaking of the sand alone and 215 Hz for lateral shaking of the 15 mm microconcrete wall alone. These observations lead us to suppose that quasi-static solutions to the 60 Hz excitation, in which phase lag is ignored, may be acceptable.

2.2 Quasi-static elastic interaction

Suppose that the elastic wall interaction problem can be solved approximately by superposing a uniform lateral acceleration field $k_h g$ onto the vertical gravitational field g, thereby ignoring phase changes. D'Alembert's principle can then be used to create a resultant body force at an angle $\beta = \tan^{-1} k_h$ to the horizontal, which can be written as $\gamma/\cos\beta$ in magnitude as shown in Figure 3(a). If the state of stress at every point along any plane HH parallel to the surface of the fill is considered unique, it must follow that the side forces E acting

on the sides of the element shown in Figure 3(a) will cancel each other. A force balance then shows that the shear and normal stresses on plane HH at a separation Z from the surface are

$$\tau = \gamma Z \tan\beta \tag{4}$$

$$\sigma = \gamma Z \tag{5}$$

The shear angle with respect to axes parallel to the wall and fill surface can then be expressed for an elastic material as $\gamma Z\tan\beta/G$. It follows that if the retaining wall boundary is regarded as transmitting no extra normal stress during the application of the lateral body force (which is equivalent to saying that its bending stiffness is negligible), whilst being fully able to respond with shear stresses complementary to those on planes HH, the local change in angle of that boundary can be written

$$\frac{dy}{dZ} = \frac{\gamma Z \tan\beta}{G} \tag{6}$$

Substituting soil parameters appropriate to modelling medium-dense soil at 80g

$$\frac{dy}{dZ} = \frac{\tan\beta \times 17 \times 80\ Z}{3 \times 10^5\ Z^{\frac{1}{2}}} = \frac{\tan\beta\ Z^{\frac{1}{2}}}{221} \tag{7}$$

which can be integrated to give a deflection of the soil surface relative to the base of the wall

$$y_s = \frac{\tan\beta}{221} \times \frac{2}{3} \times 0.175^{3/2} = \frac{\tan\beta}{4520} \tag{8}$$

If, by contrast, the model retaining wall is subject to a similar quasi-static lateral force field $K_h g$ or $g\tan\beta$ while the soil is assumed to exert unchanging normal stresses, the crest deflection is given by

$$y_w = \frac{WH^3}{8EI} \tag{9}$$

where the lateral load $W = Mng\tan\beta$ has the value 4.8 kN/m at 80g for the 15 mm wall. Substituting for parameter EI the value $B_e = 4.8\ kNm^2/m$, we obtain

$$y_w = \frac{\tan\beta}{1490} \tag{10}$$

It is apparent, therefore, that the sand backfill is roughly three times stiffer than its retaining wall, subject to the same lateral force field.

Not only are the crest deflections of the wall and soil different according to the foregoing partially uncoupled analysis, but the profile of the deflection with depth is also different as shown in Figure 3(b). If, notwithstanding the

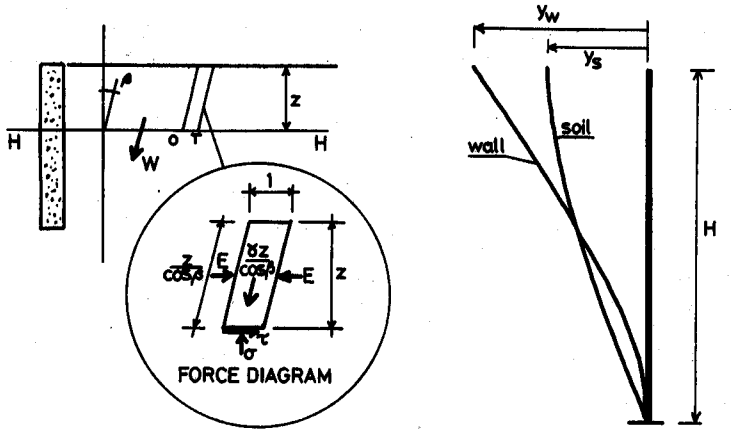

(a) lateral force field (b) partially uncoupled deflection profile

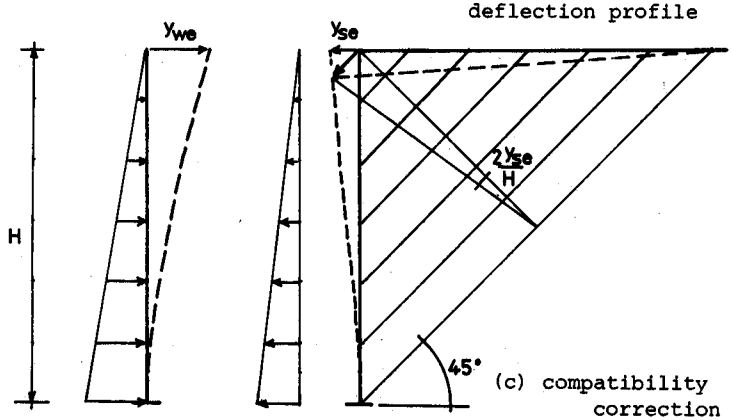

(c) compatibility correction

Fig. 3 Quasi-static elastic interaction

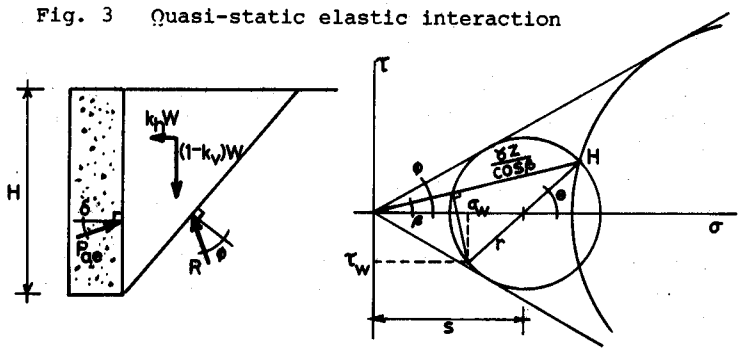

Fig. 4(a) Mononobe-Okabe forces (b) Mohr circle construction

complexity of this incompatibility, a tensile stress increment between the wall and the soil

$$\sigma_e = - K_e \gamma Z \qquad (11)$$

(arbitrarily chosen to be proportional to depth) is allowed simply to marry the crest deflections, an estimate of the actual crest deflection can be made. Consider the deformation shown in Figure 3(c), in which the cantilever tip moves towards the soil by

$$y_{we} = \frac{1}{30} \frac{K_e \gamma H^5}{B_e} \qquad (12)$$

according to bending theory, while a 45° triangle of fill deforms with a simple shear angle of 2 y_{se}/H. The shear stress increment mobilized on the 45° lines would then be

$$\tau_e = \frac{2G\, y_{se}}{H} \qquad (13)$$

which would have to be equal, by consideration of a Mohr circle of stress increments, to one half the decrement of lateral stress,

$$\tau_e = \frac{2G\, y_{se}}{H} = \frac{1}{2} K_e \gamma Z \qquad (14)$$

If we now accept $G = 1000\ Z$ MN/m^2 as a revised expression for the shear modulus of the sand in the model at 80g (which agrees only at mid-height with the previous recommended expression $300\ Z^{\frac{1}{2}}$ MN/m^2) equation 14 can be satisfied. The soil crest behind the wall is then estimated to move towards the wall a distance

$$y_{se} = \frac{1}{4} \frac{K_e \gamma H}{10^6} \qquad (15)$$

Compatibility is crudely satisfied if the sand and wall remain in contact at the crest, so that

$$y_w - y_{we} = y_s + y_{se} \qquad (16)$$

Substituting values appropriate to the elastic behaviour of the model at 80 g we then obtain

$$\frac{\tan\beta}{1490} - 0.00155\, K_e = \frac{\tan\beta}{4520} + 0.00006\, K_e \qquad (17)$$

It is therefore clear that the soil is so much stiffer than the wall in this local interaction that almost all the required correction in deflection must be contributed by the wall, so

that

$$K_e = 0.28 \tan\beta \qquad (18)$$

and the joint crest movement

$$y = \frac{\tan\beta}{4220} \qquad (19)$$

The value and purpose of this extended approximate calculation has been to demonstrate that the relative flexibility of the 15 mm model retaining wall ensures that the effective pattern of overall elastic behaviour is one of outward simple shear of the soil accompanied by marked reductions in lateral stress when the equivalent lateral force field is outwards, and by similar inward rotations coupled with increases in lateral stress when the D'Alembert forces are directed inwards. In this quasi-static elastic treatment, the role of the sand is to reduce the movements of the flexible wall by a factor of about 3, by the agency of cyclically relaxing the initial lateral stresses.

2.3 Quasi-static plastic interaction

Figure 4(a) defines the conditions used in the limiting wedge analysis of Mononobe (1929) and Okabe (1926), for the case of a rough vertical face retaining granular fill with a horizontal surface and subject to a constant horizontal acceleration g tanβ. The active thrust inclined at angle δ is deduced to be

$$Pa = 0.5\,\gamma H^2\,Ka \qquad (20)$$

where

$$Ka = \frac{\cos^2(\phi-\beta)}{\cos\beta\,\cos(\delta+\beta)}\left[1 + \left(\frac{\sin(\phi+\delta)\sin(\phi-\beta)}{\cos(\delta+\beta)}\right)^{\frac{1}{2}}\right]^2 \qquad (21)$$

The most logical interpretation of this solution is that the stress distribution on the wall is triangularly distributed with a normal component

$$\sigma_a = \gamma Z\,Ka\cos\delta \qquad (22)$$

This method was devised to predict the forces on walls whose bases were sliding. There is therefore some question whether the analysis would be relevant to the rotational failure of a wall stem about a plastic hinge, since the kinematic conditions would be quite different.

Equations 4 and 5 referred to a uniform state of stress along a horizontal surface HH, and Figure 3(a) drew attention to the analogy between the quasi-static stresses and the problem of a wall retaining a slope angle β of soil with a resultant unit weight of $\gamma/\cos\beta$. Figure 4(b) shows a Mohr circle construction in which the angle of shearing of the soil (or of the soil/wall interface) has been permitted to reach a

limiting value ϕ'. It is easily shown from this construction that

$$\sigma_a = \gamma Z \left[\frac{2 \sec\beta}{(\cos\beta + \sqrt{\sin^2\phi - \sin^2\beta})} - 1 \right] \quad (23)$$

$$\tau_a = \gamma Z \tan\beta \quad (24)$$

When typical values $\beta = 10^o$ $\phi = 40^o$, are inserted into equations 23 and 22 (taking $\delta = \phi'$) the corresponding normal stress ratios $\sigma_a/\gamma Z$ are calculated to be 0.27 and 0.34, so it is clear that estimates close to the original Monobe-Okabe values can be derived without appeal to the kinematics of sliding wedges.

3. Data of tests

3.1 Achievement of initial stresses

Figure 5 shows the crest deflection of the 15 mm model wall increasing as the acceleration was increased to 80 g with either dense or loose sand fill. Superimposed on the same axes are the relationships derived by using equation 3 with the curve-fitting parameters $B_1 = 6.0$ kNm^2/m, $M_1 = 0.08$ kNm/m for the wall and angles of shearing resistance of 50^o, 40^o, and 30^o for the sand, which has been assumed to create a triangular pressure distribution with a lateral earth pressure coefficient taken from equations 21 and 22 (with $\delta = 30^o$ and $\beta = 0$). The behaviour of the dense sand fill was broadly consistent with what is expected for 'active' soil mobilizing its full shearing resistance of $\phi' = 50^o$ at an average wall rotation of 1/875. The loose fill created an average rotation of 1/300, and it was thereby inferred to mobilize an angle of shearing resistance of 37^o. However, it may be recalled from Figure 2(b) that the deflection parameters were a relatively poor fit at large bend-moments. It happened that distinct yielding was observed in the loose sand test as 80 g was first reached, and if this alternatively is taken to mean that a limiting moment of 0.29 kNm/m was then just reached at the base, a value $\phi' = 29^o$ is inferred.

Although the sparseness of deformation and stress data in these tests leaves considerable room for doubt over the detailed accuracy of the triangular static stress assumption, it is clear that 'active' conditions were broadly achieved in both before shaking tests were attempted.

3.2 Shaking tests on non-yielding walls

Figure 6 shows the effects of the first seven cycles of base shaking of a 20% (maximum) earthquake ($\beta = 11.3^o$) on the 15 mm wall retaining dense sand. The Mononobe-Okabe expression of equation 21 and 22 may be used with $\delta = 30^o$, $\phi = 50^o$ to generate a normal earth pressure coefficient Ka $\cos\delta = 0.197$ which would

imply a total crest deflection of 0.70 mm in comparison to the greatest observed deflection of 0.58 mm (0.20 mm initial + 0.38 mm during the seventh pulse). The base acceleration at the seventh cycle was only 15% ($\beta = 8.5^{o}$) which, if used in the same analysis, would have given a predicted maximum displacement of 0.56 mm.

The approximate elastic analysis leading to equation 19 provides an estimate of 0.035 mm for the amplitude of crest displacement expected if the peak acceleration coefficient were 15%, compared with the measured amplitude of 0.038 mm on the seventh cycle.

It may be concluded that the quasi-static analyses provide quite reasonable estimates of deflection in this case. The build-up over seven cycles must presumably be due to inertial effects, in that some fraction of the potential outward force in early cycles must be dissipated in creating the required outward mass-accelerations. It may also be noted that the delay of circa 1.5 milliseconds between the traces of the crest and base accelerometers is not inconsistent with our understanding of the speed of propagation from the boundaries.

3.3 Shaking tests on yielding walls

Figure 7 shows the effects of the first twelve cycles of base shaking of a 20% (maximum) earthquake on the 15 mm wall retaining loose sand. It is evident that the build up of the ultimate deflection of 3.5 mm requires 12 cycles. It is hardly surprising that the outward throw on the first full cycle is limited to 1 mm since the amplitude of the base shaking is itself only 1.1 mm at 20% acceleration. The slow build-up may therefore be attributed mainly to the large ratio between the final outward deflection and the earthquake amplitude. The base acceleration in the twelvth cycle is 12.5% ($\beta = 7.1^{o}$), and the corresponding Mononobe-Okabe estimate of the base bending moment with $\delta = 30^{o}$, $\phi = 35^{o}$ is 0.31 kNm/m compared with the maximal value of 0.29 kNm/m measured in the static tests. This good agreement also correlates with the observation that when the base acceleration of earlier cycles exceeded 12.5% that of the wall crest and its fill exhibited a cut-off at precisely this value, the wall stem being unable to deliver any more than the 0.3 kNm/m required to deliver these mass-accelerations.

The amplitude of alternating crest deflection at the twelfth cycle is 0.050 mm. The predicted amplitude of elastic vibration from section 23 becomes 0.030 mm. That estimate would have been greater if the likely reduction of dynamic modulus at these lower densities had been taken into account. Once again, the simplified quasi-static treatment has been sufficient to describe every aspect of the behaviour except for the initial phase in which inertia effects and the limited magnitude of base deflections compared with potential crest deflections

causes a slowing in the rate of build-up of permanent strains.

4. Conclusions

1. The detailed prediction of lateral pressures on retaining walls, whether dynamic or static, has been demonstrated again to be chiefly a function of the angle of shearing resistance of the soil. The Monobe-Okabe method of quasi-static wedge analysis has been shown to be quite accurate in the prediction of maximum deflections, within the limits of particular tests on flexible microconcrete retaining walls.

2. An approximate quasi-static elastic analysis has been constructed which offers a view of the interaction between the wall and the soil as chiefly comprising simple shear of the rectangular block of soil fill. Many cantilever walls will prove to be much more flexible than the soil they retain, should that soil remain elastic, so that their tendency in an earthquake will be to deform more than the soil. This tendency can be counteracted by the ensuing de-stressing of the soil-wall interface, so that the effect of the presence of an elastic soil fill is to reduce lateral deflections of a shaken wall. The predictions of oscillating deflections by the approximate elastic theory appeared from the model test results to be broadly correct.

3. A feature of the model test results was the progressive build-up of the permanent (plastic) deformation over a number of cycles. The quasi-static analyses took no account of the transient inertial effects, by which some of the available lateral force must be consumed in creating mass accelerations. An avenue worth exploring in the case of collapsed models will be the balance between the energy input per cycle in shaking the base and the energy absorbed per cycle in deforming the plastic hinge. Either kinematic or energy treatments should prove capable of replicating the progressive nature of plastic deformations.

4. Some pointers for discussion by retaining wall designers may be derived.

a) Retaining walls can be proof-loaded in order to guarantee serviceability up to an agreed seismic condition. Mononobe-Okabe stresses can be calculated and replicated statically by heavy compaction machines. The outward deflection of the wall during backfilling can be monitored as a pressure indicator. If shaking occurs in service of severity less than that allowed for in design, the interaction will be elastic. The effect of granular fill will then be to reduce the amplitude of rotation of a flexible wall to roughly $\gamma Z \tan\beta/G$ or perhaps of the order of $\tan\beta/600$, with negligible permanent deformation.

b) Retaining walls in earthquake areas should be designed to withstand severe energy inputs, and should be capable of gross deformation without rupture about a plastic hinge at their base. An estimate of the required deformation may be made by assuming that each cycle of a severe prototype earthquake could cause an increment of crest deflection equal to its own amplitude. In order that reinforced concrete be sufficiently tough to suffer rotations of the order of 5 to 10^{o} it may be necessary to use PVC sheaths to de-bond perhaps 1 m lengths of selected large diameter, round, ductile mild steel reinforcing bars at the base of the stem, so that a sufficient volume of steel is brought to failure in a catastrophic earthquake.

REFERENCES

Elms, D. G. and Richards, R. (1979) Seismic design of gravity retaining walls, Bulletin of New Zealand National Society for Earthquake Engineering.

Graff, K. F. (1975) Wave motion in elastic solids, Clarendon Press, Oxford.

Lai Cho Sim and Berrill, J. B. (1979) Shaking table tests on a model retaining wall, South Pacific Regional Conf. on Earthquake Engineering, Wellington, New Zealand.

Mononobe, N. and Matsuo, M. (1929) On the determination of earth pressures during earthquakes, Proc. World Engineering Congress, Vol. 9.

Morris, D. V. (1979) The centrifugal modelling of dynamic soil-structure interaction and earthquake behaviour, Ph.D. Thesis, Cambridge University.

Newmark, N. M. (1965) Effects of earthquakes on dams and embankments, Geotechnique 15, No. 2, pp 139-160.

Okabe, S. (1926) General theory of earth pressures, Journal, Japan Society of Civil Engineers, Vol. 12, No. 1.

Ortiz, L. A., Scott, R. F. and Lee, J. (1981) Dynamic centrifuge testing of a cantilever retaining wall, Report, Soil Mechanics Laboratory, California Institute of Technology, Pasadena, California.

Schofield, A. N. (1980) Cambridge University Geotechnical Centrifuge Operations, Geotechnique 30, No. 3, pp 227-268.

Stroud, M. A. (1971) Sand at low stress levels in the S.S.A., Ph. D. Thesis, Cambridge University.

Wood, J. H. (1973) Earthquake-induced soil pressures on structures, Ph. D. Thesis, California Institute of Technology, Pasadena, California.

Wood, J. H. (1975) Earthquake-induced pressures on a rigid wall structure, Bulletin of the New Zealand National Society for Earthquake Engineering, Vol. 8, No. 3, pp 175-186.

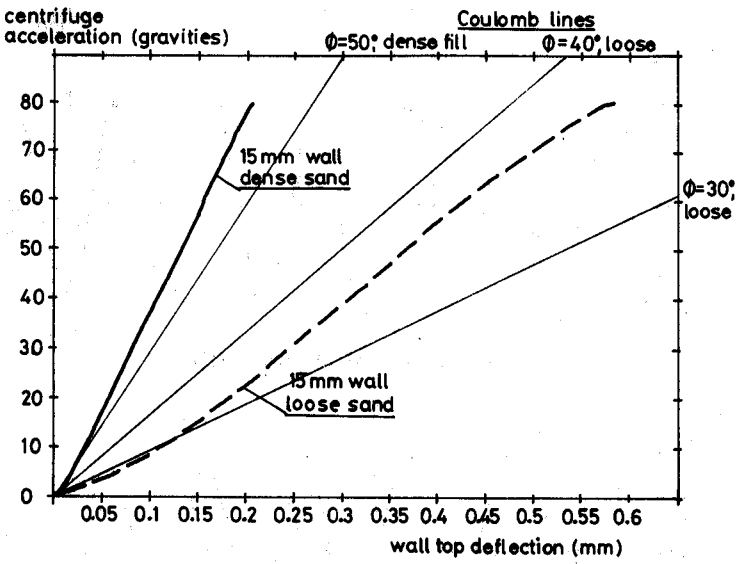

Fig. 5 Wall crest deflection with increasing centrifuge acceleration

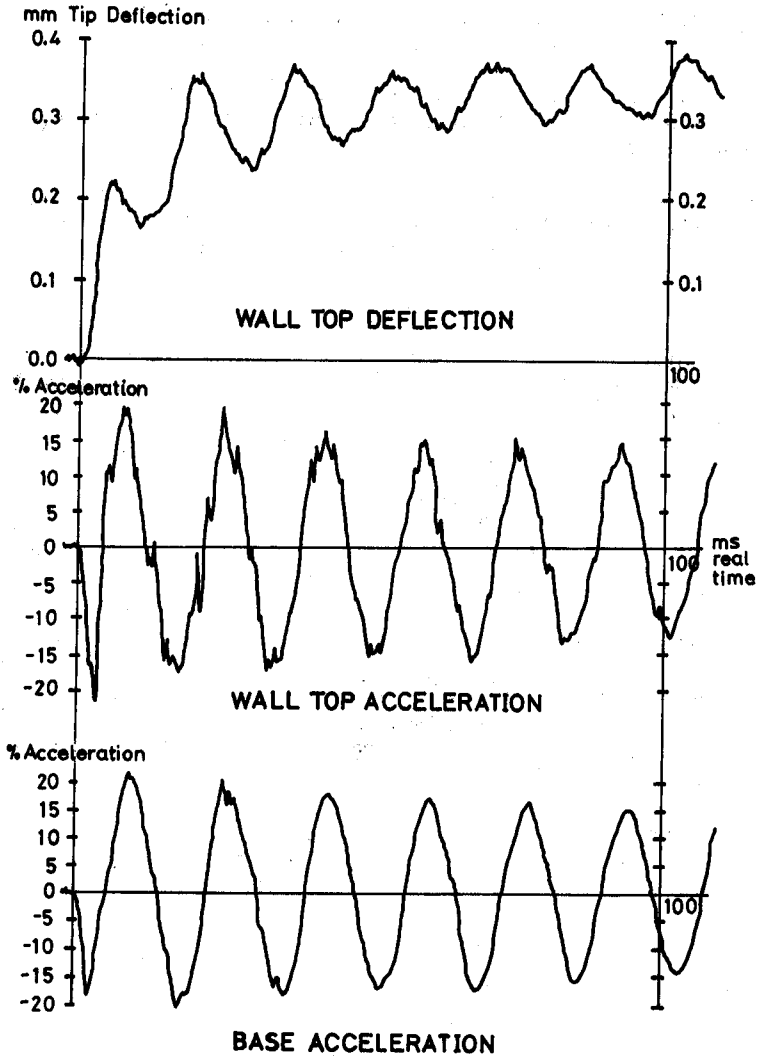

Fig. 6 20% earthquake on a non-yielding wall, dense sand backfill

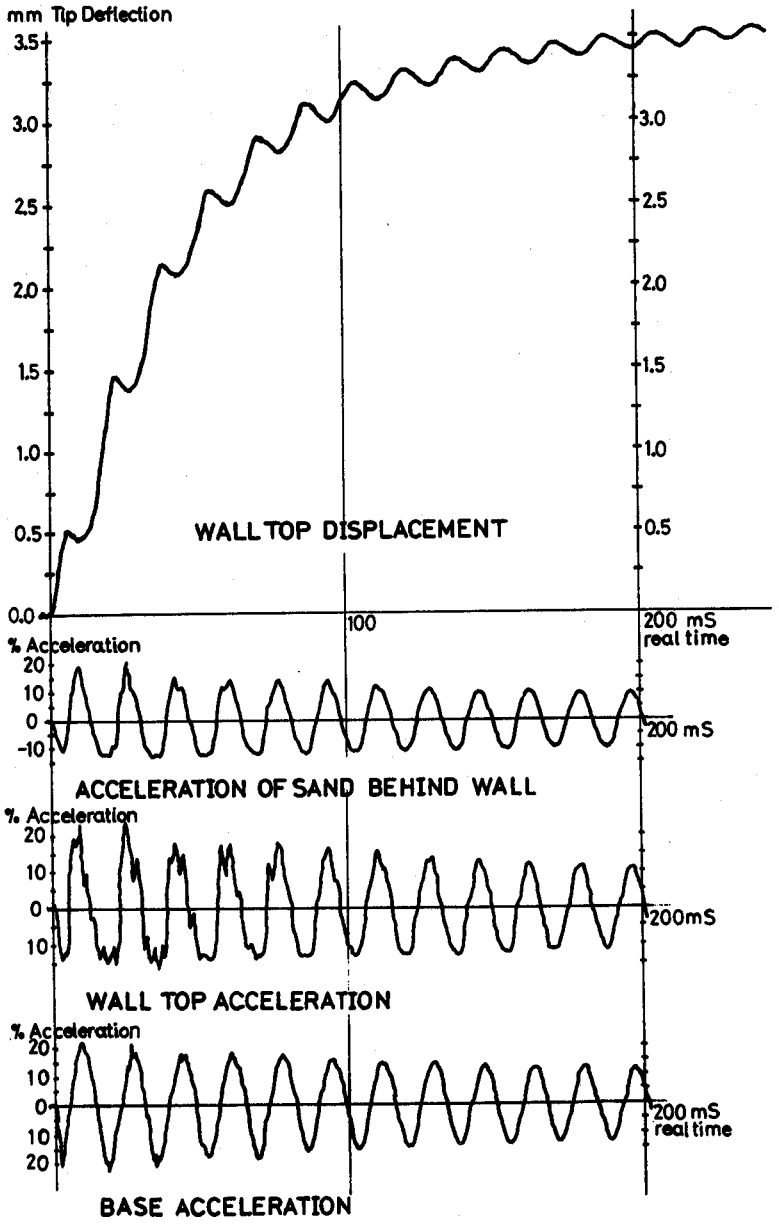

Fig. 7 20% earthquake on a yielding wall, loose sand backfill